Supporting Information

Supramolecular assembly of novel green fluorescent protein chromophore-based analogue and its application in fluorescence anti-counterfeiting

Content

1.Experimental

1.1 Materials and reagents

All chemicals and solvents are commercially available and can be used without further purification unless otherwise indicated. All the reactions took place in a dry nitrogen atmosphere, and the temperature was measured externally. The synthesized compounds were carried out by thin layer chromatography on silica gel (Hailang, Qingdao, China). Column chromatography was performed on silica gel (200-300 mesh, Qingdao Hailang, China). Minimum eagle medium was obtained from Hyclone and fetal bovine serum was obtained from Bovogen Biologicals Pty Ltd.The absorption and fluorescence spectra were determined in a quartz test tube (1cm×1cm, volume 3.5 mL). Pure water is prepared from ultra-pure water (18 MΩ*cm). The probe solution was prepared by dissolving the probe in HEPES solution (containing 1%DMSO). The probe solution was stored at 0℃ away from light.

1.2 Instrumentation

^{1}H and ^{13}C NMR Spectroscopy. In all experiments, ^{1}H and ^{13}C spectra were recorded using a Bruker Avance-400 FT nuclear magnetic resonance (NMR) spectrometer at room temperature (about 25 ℃).

High resolution mass spectroscopy. Electrospray ionization (ESI) mass spectra were obtained using a Agilent 6545 Q-TOF.

UV-vis absorption and fluorescence emission spectra. The UV-vis absorption spectra and fluorescence spectra of the compounds were determined by Hitachi U-3900 UV/visible spectrometer and Hitachi F-7000 fluorescence spectrometer, respectively.

Fluorescent anti-counterfeiting image acquisition equipment. Portable equipment such as **CA** acquisition camera system and CB[7] assembly system were designed by ourselves. Detailed parameters are semiconductor laser (λ = 445±5 nm, 10 W) for irradiation, using Huawei nove5z mobile phone camera (pixel 2340×1080) for photography, filter cut-off below 500 nm, 500 nm pass, cut-off rate od3-od4.

1.3 Synthetic procedures

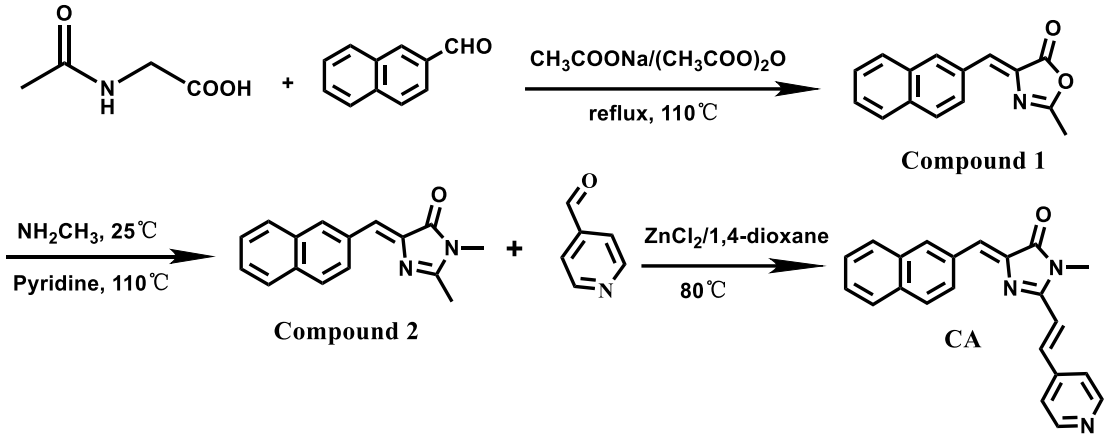

Scheme S1. Synthesis of target probes **CA**.

Synthesis of compound 1:

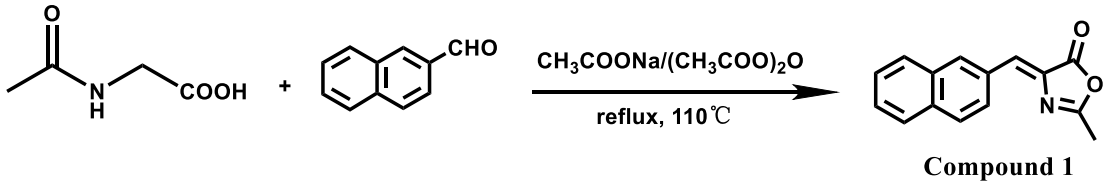

N-acetylglycine (587 mg, 0.5 mmol), 2-naphthaldehyde (781 mg, 0.5 mmol), sodium acetate (622.5 mg, 0.75 mmol) and acetic anhydride (7 mL) were added to a 50 mL round bottom flask. The mixture was stirred at 110 ºC under nitrogen atmosphere for 5 hours. After cooling to room temperature (about 25 ºC), water/ethanol mixture (2/1, v/v, 50 ml) was added. The mixture is stirred under an ice water bath for 30 minutes, filtered in a vacuum, and washed with ethanol at the same time to obtain a yellow solid. Then the product was dried overnight in a vacuum drying oven at 50 ºC to provide the compound 1 as yellow solid (924 mg, yield 78%).

Synthesis of compound 2:

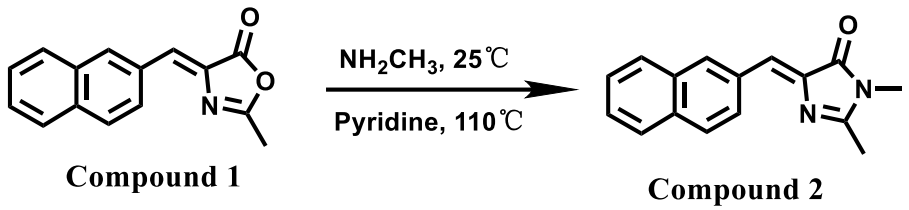

Compound 1 (100 mg, 0.42 mmol) was dissolved in methylaminoethanol containing 30% methylamine (4 ml, containing 30% methylamine) and stirred for 2 hours under the protection of nitrogen at 25 ºC. After the reaction was completed, the solvent was evaporated under pressure to obtain a white residue. 5 mL of pyridine was added to the solid and reflux was performed at 110 ºC for 8 hours. After the reaction is complete, the solvent is evaporated under pressure. The crude was purified by column chromatography (petroleum ether: ethyl acetate: 5:1-2:1) to obtain yellow solid compound 2 (59 mg, yield 56%).^{1}H NMR (400 MHz, $CDCl_3$) δ 8.44 (d, J = 9.8 Hz, 2H), 7.89 (d, J = 9.3 Hz, 1H), 7.85 (d, J = 8.6 Hz, 1H), 7.81 (d, J = 7.2 Hz, 1H), 7.53 – 7.45 (m, 2H), 7.26 (s, 1H), 3.18 (s, 3H), 2.39 (s, 3H).^{13}C NMR (101 MHz, $CDCl_3$) δ 170.85, 162.64, 138.94, 134.04, 133.35, 133.26, 132.06, 129.02, 128.44, 128.25, 127.79, 127.53, 127.51, 126.47, 26.72, 15.82.HRMS (ES+, m/z): calc. for $C_{16}H_{14}N_2O$: 251.1140, found: 251.1186.

Synthesis of probe CA:

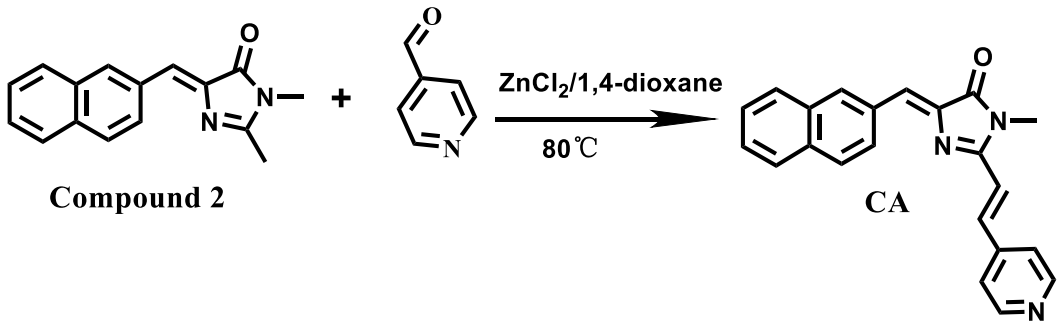

Compound 2 (381.9 mg, 1.52 mmol), 4-pyridine-formaldehyde (220 μL, 2.34 mmol) and zinc chloride (0.6 g, 4.4 mmol) were dissolved in 1, 4-dioxane (5 ml). The

reaction was stirred at 80 ºC and stirred for 3 hours under nitrogen protection. Until the TLC indicated that the starting compound 2 had disappeared, the reaction was stopped. The solvent was removed by a rotary evaporator to provide the crude products, which were further purified by column chromatography with an eluent of PE/EA (v/v = 10/1). The final pure product **CA** was obtained (301.7 mg, yield 57%). ^{1}H NMR (DMSO-d_6, 400 MHz) δ_H 8.71 (1H, s), 8.69 (2H, d, J = 6.0 Hz), 8.63 (1H, d, J = 8.8 Hz), 8.06 (1H, d, J = 15.8 Hz), 8.02 (1H, s), 7.98 (1H, d, J = 8.4 Hz), 7.94 (1H, d, J = 6.8 Hz), 7.86 (2H, d, J = 6.0 Hz), 7.62-7.56 (2H, m), 7.53 (1H, d, J = 15.8 Hz), 7.26 (1H, s), 3.32 (3H, s); ^{13}C NMR (DMSO-d_6, 101 MHz) δ_C 170.4, 162.6, 150.8, 142.6, 140.1, 138.2, 133.9, 133.8, 133.3, 132.6, 129.3, 128.7, 128.3, 127.2, 126.7, 122.6, 119.1, 27.1. HRMS (ES^+, m/z): calc. for $C_{22}H_{17}N_3O$: 340.1405, found: 340.1446. HRMS (ES+, m/z): calc. for $C_{22}H_{17}N_3O$: 340.1405, found: 340.1454.

2. Additional Information

2.1 Fluorescent anti-counterfeiting imaging device

Portable camera system for capturing images in Fluorescent anti-counterfeiting assay on A4 papers was similar as the portable system in our previous work.[1] The power supply is made from rechargeable lithium-ion batteries. The detailed parameters are semiconductor laser (λ = 445±5 nm, 10 W) for irradiation, Huawei nova 5z smart phone camera (pixel 2340 × 1080) was used for photography, optical filter was optical longpass filter that was used for transmission wavelength more than 500 nm, the cut-off rate is OD5.

2.2 pH effect on the absorption and fluorescence of CA

First, the photophysical properties of **CA** in pure water were studied by UV-Vis spectrum and fluorescence emission spectrum. We investigated the effect of pH on UV absorption and fluorescence of **CA** (50 μM) at different pH values (pH is at the range of 3.30-10.83). Initially, pH titration was performed in pure water. The UV absorption and fluorescence emission of **CA** did not change significantly at different pH values. The maximum absorption of **CA** is at 425 nm and the maximum fluorescence emission

is at 535 nm. The results showed that pH did not affect on the probe **CA**.

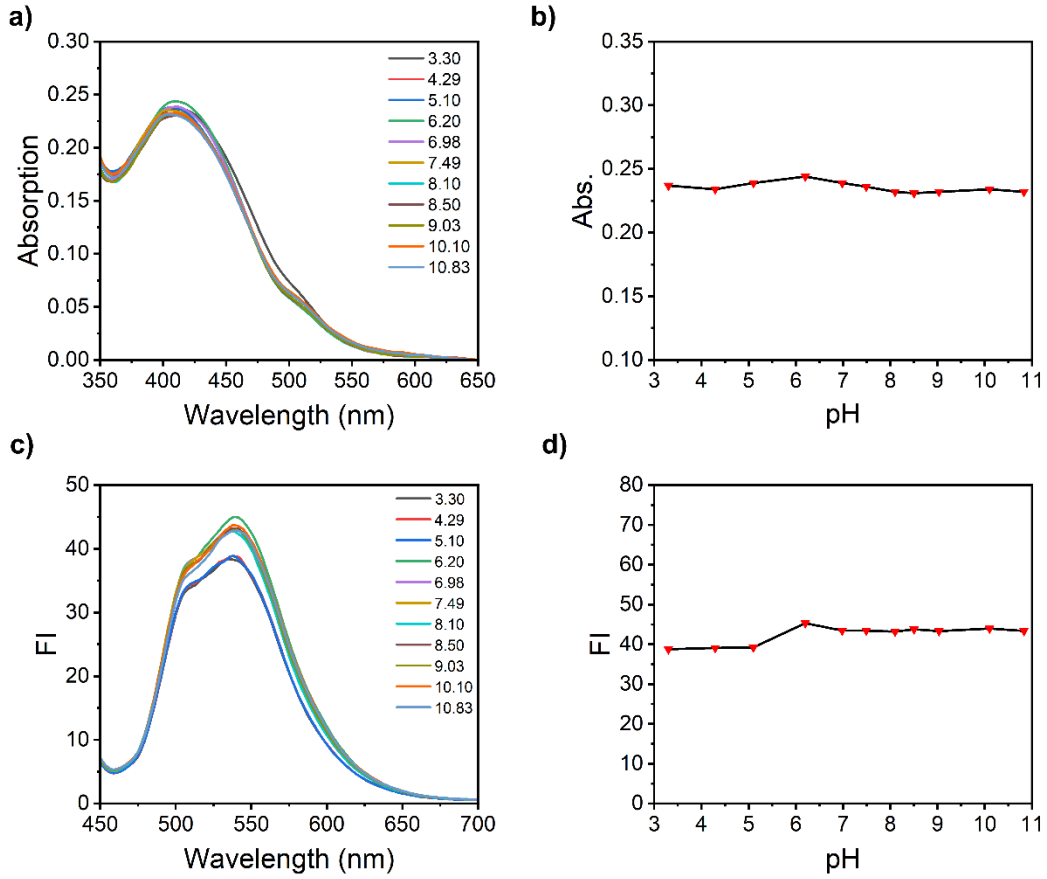

Fig. S1 (a) UV absorption spectra of target probe **CA** (50 μM) at different pH in pure water. (b) Scatter diagram of maximum UV absorption value (pH 3.30-10.83). (c) fluorescence spectra of target probe **CA** (50 μM) at different pH in pure water. (d) Scatter diagram of fluorescence emission spectra (pH 3.30-10.83). λ_{ex} =425 nm. Slit widths ex=5 nm and em=5 nm.

2.3 UV absorption of CA after addition of CB[6], CB[7] and CB[8]

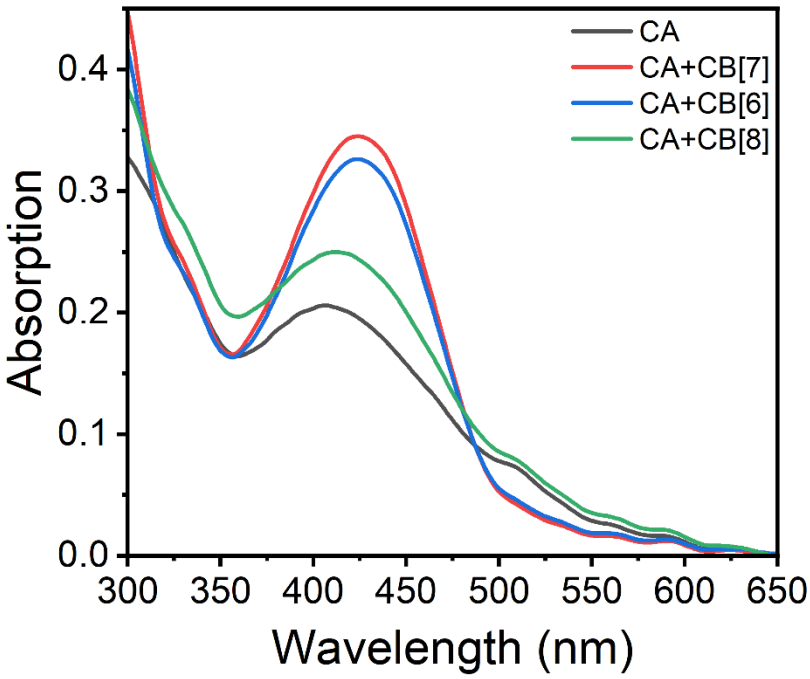

Fig. S2 Absorption spectra of 100 μM CB[6], CB[7] and CB[8] were added to 50 μM **CA** (HEPES buffer containing 1% DMSO as a co-solvent), respectively. λ_{ex} =425 nm. Slit widths ex=5 nm and em=5 nm.

2.4 The isothermal titration calorimetry test of interaction between CA and CB[6] (or CB[8])

Isothermal titration calorimetry. The affinity between **CA** and CB[6]/CB[8] was determined by NANO-ITC isothermal titration calorimetry (ITC). All titrations were performed at 25°C and in HEPES solution containing 10%DMSO. CB[6]/CB[8] (100 μM) was dropped into **CA** solution (10 μM) at 2 μL for 25 times, the drop interval was 120 s, and the stirring speed was 350r/min. As a reference run, CB[6]/CB[8] was titrated into HEPES solution of **CA**, and CB[6]/CB[8] was titrated into a blank solvent (containing 10%DMSO HEPES solution) in the control group. The resulting heat map is calibrated at baseline and the combined signal is calibrated for control measurements. The test data were fitted with an independent model, and the corresponding dissociation

constant K_d (reciprocal of the binding constant K_a), stoichiometric ratio n, enthalpy change ΔH, entropy change ΔS and other parameters were obtained (Table 1). In the ITC measurement process, CB[8] titrated CA process showed no obvious heat change, indicating no binding effect, while CB[6] titrated CA process showed remarkable heat change (endothermic), indicating the existence of binding effect. The ITC curve shows that the stoichiometric ratio of probe **CA** and CB[6] complex is 1:1 (**CA**/CB[6]). The binding constant is determined as $K_a = 3.6 \times 10^4$ [that is, the dissociation constant (K_d) = 2.77×10^{-5}], ΔH is 100 kJ/mol, ΔS 422.6 J/mol·K, ΔH > 0, ΔS > 0, which is the binding process driven by hydrophobic action (Fig. S3, S4).

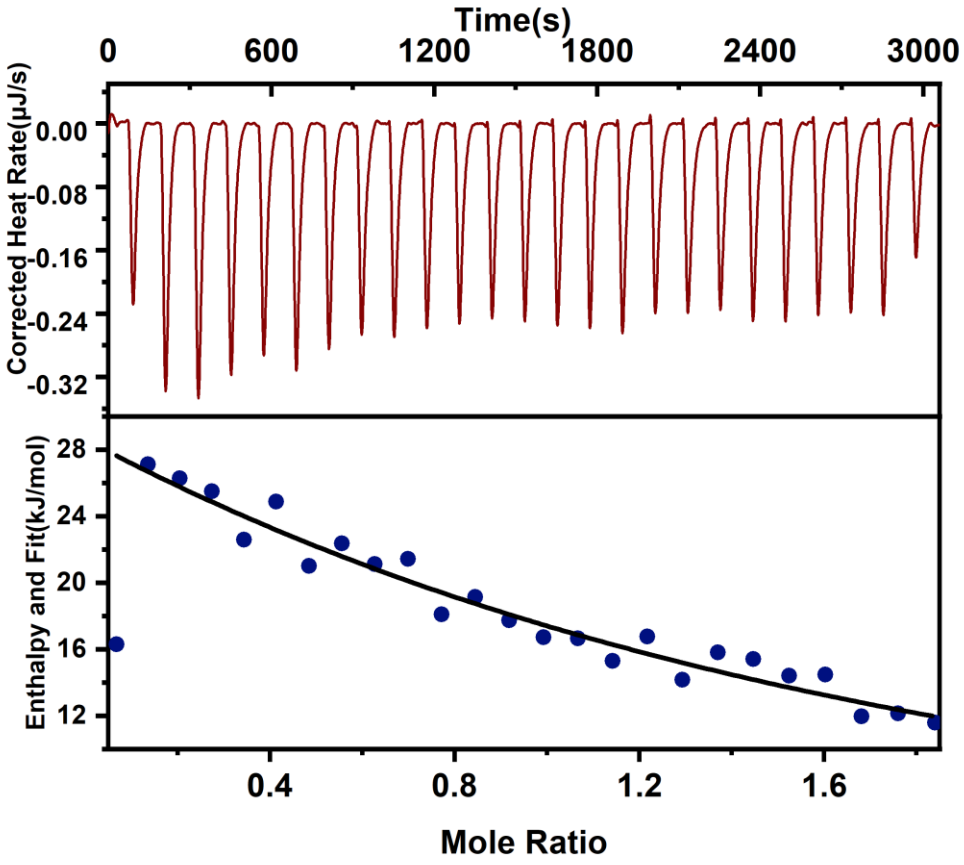

Fig. S3 ITC thermal image: Corrected Heat Rate (figure above after data correction); Combined heat: A fitting curve titrated from 100 μM CB[6] to 10 μM **CA** in HEPES solution at 25 ºC.

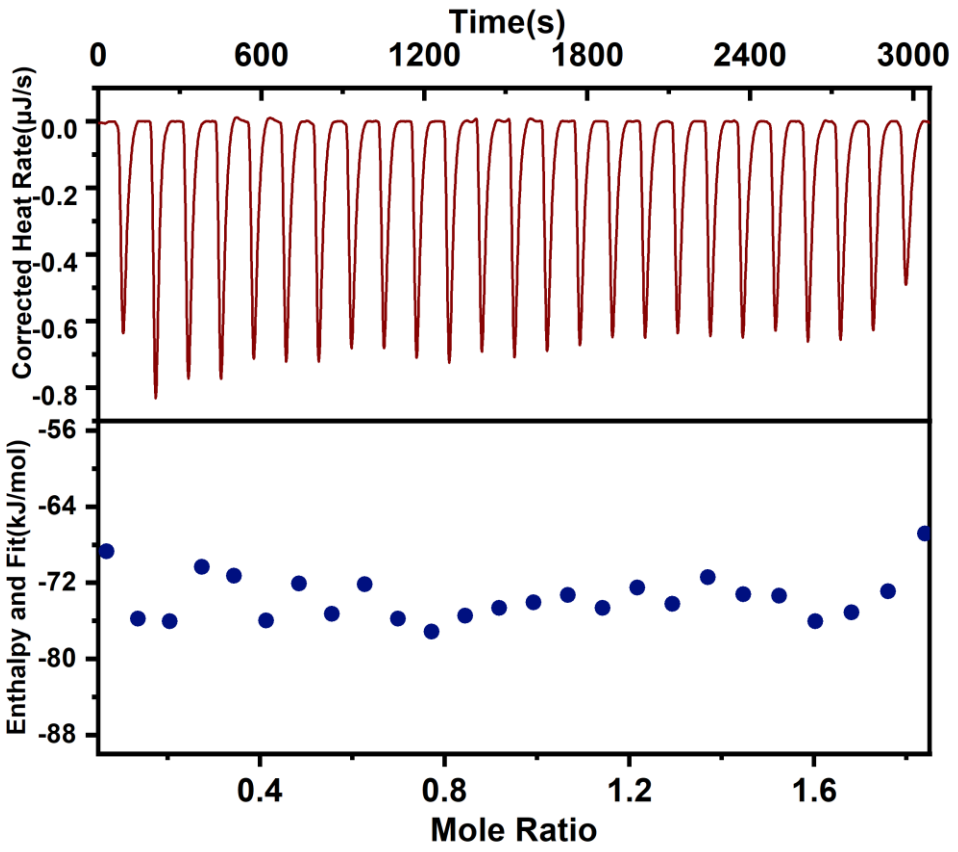

Fig. S4 ITC thermal image: Corrected Heat Rate (figure above after data correction); Comprehensive heat: The scatter diagram (experiment, figure below) in a solution of 100 μM CB[8] titrated to 10 μM **CA** at 25 ºC shows no binding phenomenon.

2.5 Dynamics interaction between CA and CB[6]

In the real-time dynamic test of interaction between **CA** on CB[6], a fluorometer is used to conduct in time-scan mode. CB[6] is not added at the beginning, and the scan is performed for first 20 seconds. At this time, the fluorescence intensity signal is very weak. At 20-second time point, different concentration of CB[6] was added immediately, and the fluorescence intensity increased (10-50 μM). The fluorescence intensity reached a plateau after the concentration of CB[6] above 50 μM (50-80 μM). The fluorescence intensity remained stable during 20s. Then, the fluorescence intensity immediately decreased after amantadine hydrochloride was added (the binding constant between amantadine hydrochloride and CB[6] could reach $K_a = 10^{12}$. It has a stronger

binding affinity towards CB[6], thereby replacing **CA** from the cavity of CB[6]. From the fitting plot between the fluorescence intensity and molar ration of CB[6] versus **CA** in Fig. S5b, we can deduce that **CA** and CB[6] is assembled into 1:1 host-guest (CB[6]-**CA)** complex.

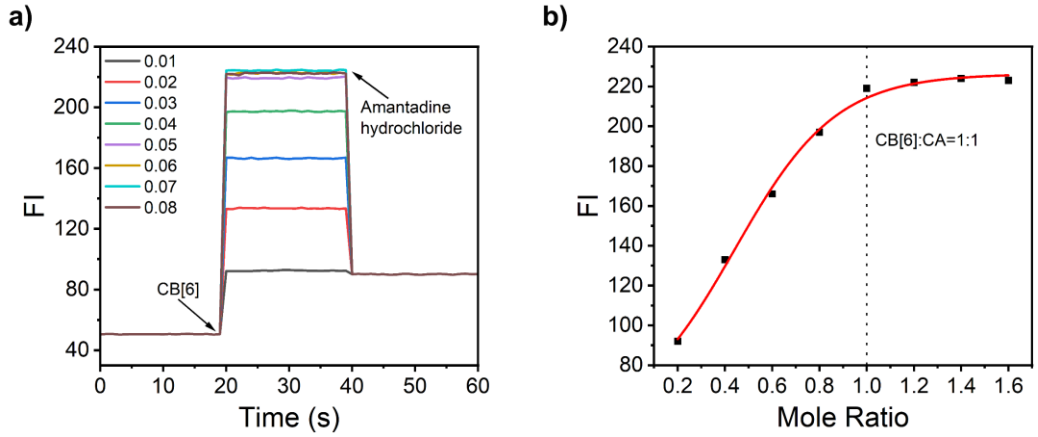

Fig. S5 (a) Changes in the emission intensity (λ_{ex}= 425 nm, λ_{em} = 535 nm) upon addition of varying concentrations of CB[6] (10-80 μM) into 50 μM **CA**, and followed by addition of amantadine hydrochloride (50 μM) in 100 mM HEPES, pH 7.4, 25 °C. (b) Resulting fluorescence intensity and fitted plot for CB[6] : **CA** molar ratio. Slit widths ex=5 nm and em=5 nm.

2.6 UV-Vis absorption changes upon addition of increased concentration of CB[7]

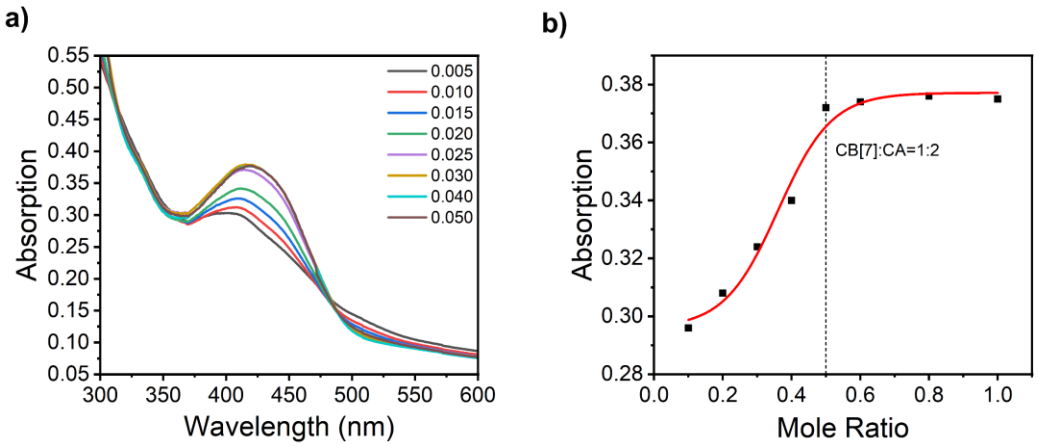

Fig. S6. a) UV-Vis absorption changes of **CA** (50μM) by gradually adding CB[7] solution (5-50 μM) in HEPES solution (containing 1% DMSO). b) Fitted plot of resulting absorption intensity to CB[7]:**CA** molar ratio according to the results in (a).

2.7 Other potential influence on probe CA and CA-CB[7] system

2.7.1 The interaction between β- cyclodextrin (or γ- cyclodextrin) and probe CA

The assay was conducted to evaluate the fluorescence enhancement of **CA** after addition of β-cyclodextrin (and β-CD) or γ-cyclodextrin (γ-CD), respectively. As shown in **Fig. S7**, β-CD (or γ-CD) cannot enhance the fluorescence intensity of **CA**. There are no remarkable changes were observed from the absorption spectra.

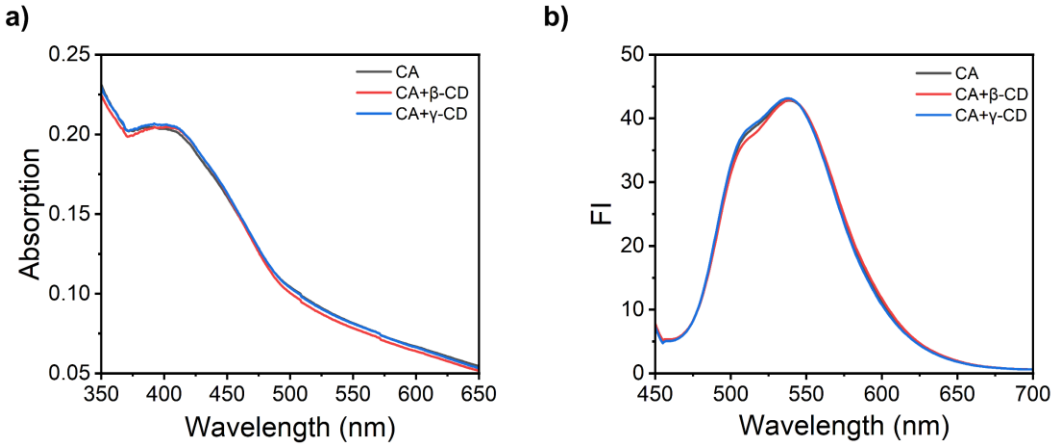

Figure S7. (a) UV changes of **CA** (50 μM) before and after addition of 50 μM β-cyclodextrin (or 50 μM γ-cyclodextrin), respectively. (b) Fluorescence changes of **CA** (50 μM) before and after addition of 50 μM β-cyclodextrin (or 50 μM γ-cyclodextrin), respectively. λ_{ex} =425 nm. Slit widths ex = 5 nm and em = 5 nm.

2.7.2 The effects of 1-adamantane methylamine, methylamine, ethylenediamine and 3-hydroxytyramine on the CA-CB[7] complex

The effects of adamantane, 1-adamantane methylamine, methylamine, ethylenediamine, and 3-hydroxytyramine on the fluorescence changes of **CA**-CB[7] complex were tested. Firstly, the fluorescence of 50 μM **CA** in HEPES solution and **CA**-CB[7] system (adding 25 μM CB[7] to 50 μM **CA** in HEPES solution) were tested, respectively. After addition of 50 μM adamantane, 1-adamantane methylamine, methylamine, ethylenediamine, 3-hydroxytyramine and amantadine hydrochloride, respectively, to the **CA**-CB[7] system, the fluorescence was further recorded. The results showed the high specificity of 1-adamantanamine hydrochloride for the disassembly process of

CA-CB[7] complex.

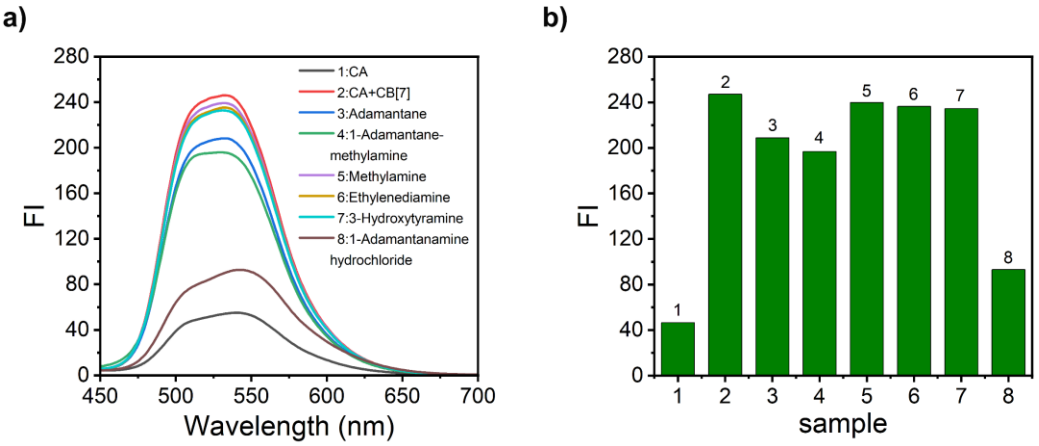

Fig. S8. (a) Fluorescence intensity of **CA**, **CA**-CB[7], and **CA**-CB[7] solutions with addition of 1-adamantane methylamine, methylamine, ethylenediamine and 3-hydroxytyramine, respectively. (b) The relatively fluorescence intensity according to maximum emission from (a). λ_{ex} =425 nm. Slit widths ex=5 nm and em=5 nm.

2.8 Fluorescence lifetime assay of CA, CA-CB[7] and CA-CB[7]-amantadine hydrochloride systems

A fluorescence lifetime assay of **CA**, **CA**-CB[7] and **CA**-CB[7]-amantadine hydrochloride system was conducted. As shown in **Fig. S9**, time-dependent fluorescence experiments with time-correlated single photon counting (TCSPC) was performed to teste the lifetime of **CA**, **CA**-CB[7] and **CA**-CB[7]-amantadine hydrochloride systems in HEPES buffer. The results showed the average lifetime of **CA** is ~ 19 ns, the average lifetime of **CA**-CB[7] system is ~ 27 ns, and the average lifetime of **CA**-CB[7]-Amantadine hydrochloride system is ~ 20 ns. [2, 3]

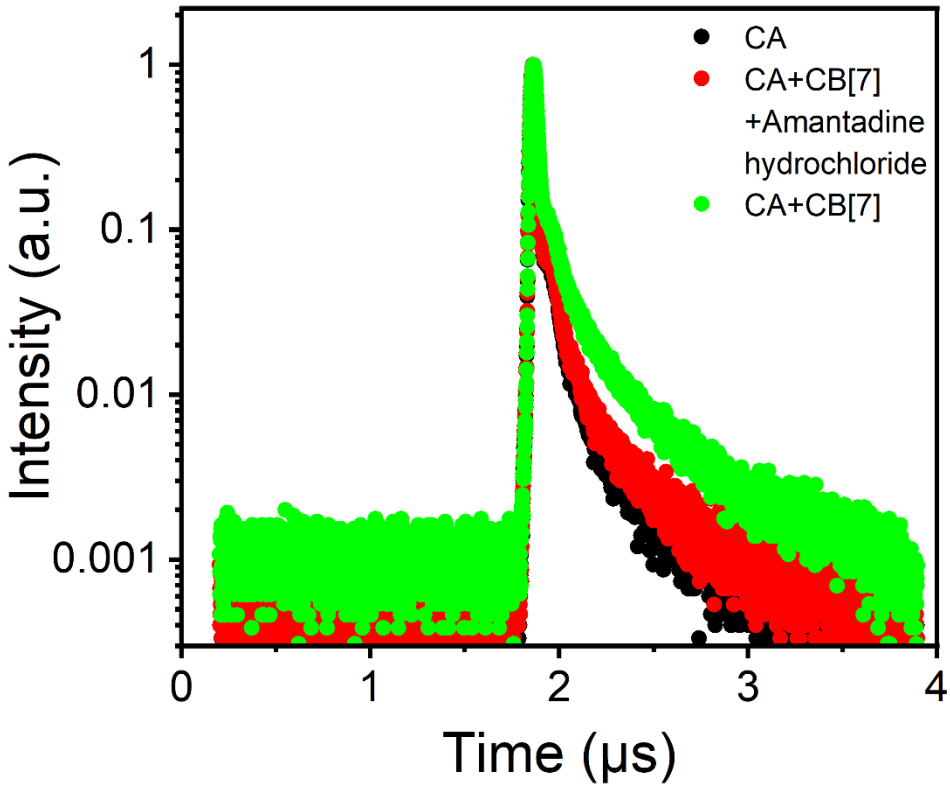

Fig. S9 Fluorescence lifetime assay of **CA**, **CA**-CB[7] and **CA**-CB[7]-Amantadine hydrochloride system.

2.9 Fluorescence quantum yields of CA and CA-CB[7] complex

The fluorescence quantum yields of **CA** and **CA**-CB[7] in HEPES were determined using Rhodamine 6G in pure water (Φ = 0.90) as a reference[4]. The quantum yield of **CA** and **CA**-CB[7] in HEPES solution at 25°C was then calculated. The relative fluorescence quantum yields (Φ) were measured on optically dilute samples (absorbance < 0.05) which were degassed by bubbling with oxygen-free nitrogen.

$$\Phi_{sample} = \Phi_{standard} \left(\frac{\mathrm{Grad}_{sample}}{\mathrm{Grad}_{\mathrm{standard}}}\right) \left(\frac{\eta^2_{\mathrm{sample}}}{\eta^2_{\mathrm{standard}}}\right)$$

Where **Φ** (sample) is the relative fluorescence quantum yield of **CA** and **CA**-CB[7] in HEPES buffer, respectively. And **Φ** (standard) is the fluorescence quantum yield of Rhodamine 6G in pure water (**Φ** = 0.90). Grad (standard) and Grad (sample) are the gradients from the plot of integrated fluorescence intensity *vs* absorbance (absorbance

< 0.05). Grad (standard) was calculated to be 1524969 and Grad (samples) were calculated to be 27210 for CA, and 223583 for CA-CB[7] system, respectively. The η (standard) and η (sample) are the refractive indexes of the solvents. Herein, η (standard) and η (sample) is as the same value.

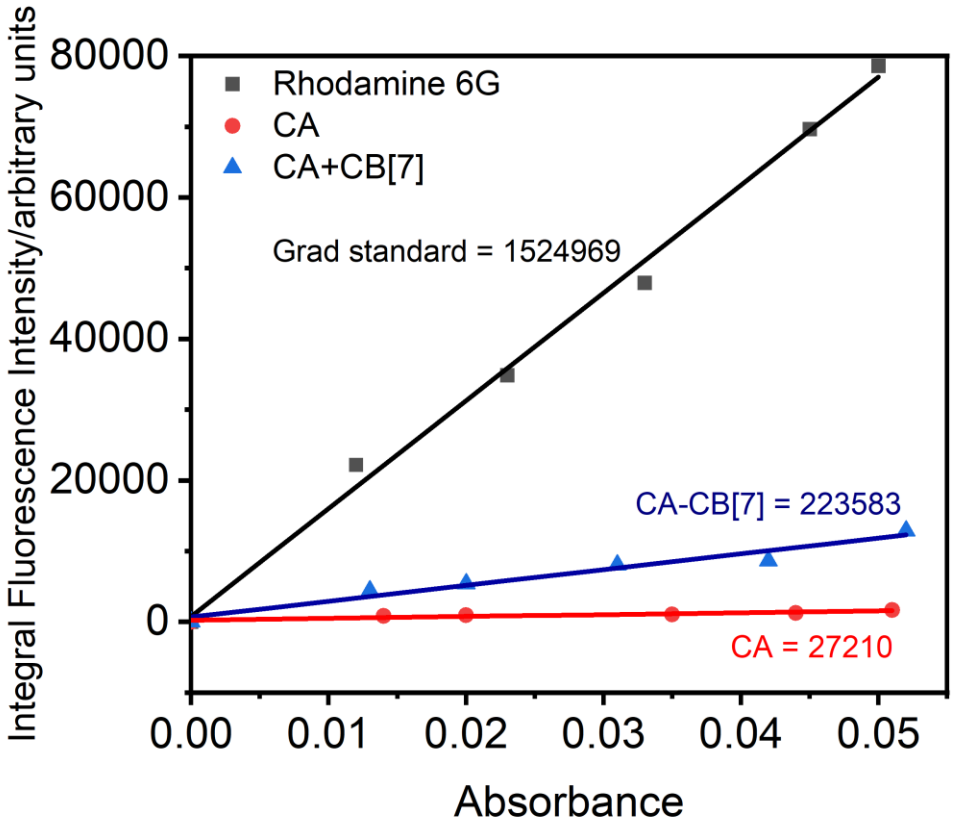

Fig. S10 Plots of integrated fluorescence intensity *vs* absorbance for **CA**, **CA**-CB[7] in HEPES buffer, and Rhodamine 6G in H_2O, respectively.

Table S2. Fluorescence quantum yields for **CA** and **CA**-CB[7].

	Fluorescence quantum yields (Φ)
CA	0.02
CA-CB[7]	0.13

3. The anti-counterfeiting properties of the CA-CB[7] system

3.1 The fluorescent anti-counterfeiting property of only CA without CB[7]

We carried out the assay of anti-counterfeit property of only **CA** without CB[7]. The characters of **CA** were written with the HEPES buffer solution, and then apply it with the **CA** solution. The information is not displayed under semiconductor lasers (λ = 445 ± 5 nm, 10 w).The result showed that only **CA** without CB[7] does not have a fluorescent anti-counterfeiting effect.

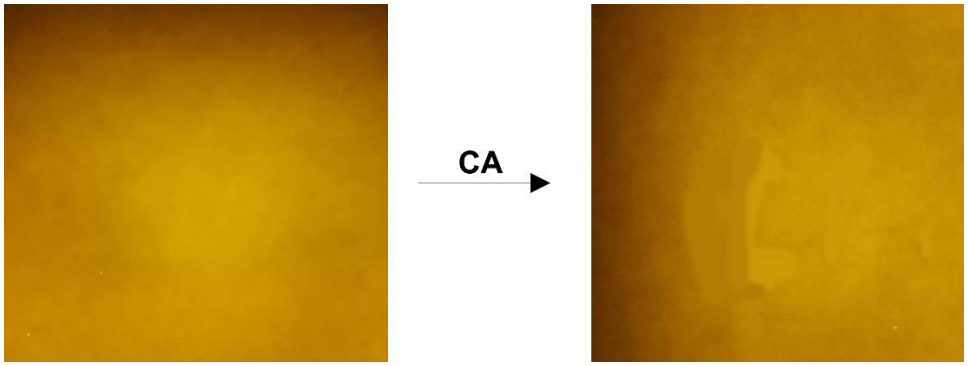

Fig. S11 The fluorescent anti-counterfeiting effect of only **CA** without CB[7].

3.2 The fluorescence stability and durability of patterns visualized by CA-CB [7] system

We have conducted the assay to evaluate the stability and durability of the fluorescence of **CA**-CB[7] complex under real-world conditions (e.g., exposure to light, humidity, physical abrasion, or different temperatures) to explore the potential practical use. All the results showed that the stability and durability of the **CA**-CB[7] complex were good. A4 paper was cut into the shape of a “star” pattern. **CA**-CB[7] system was used for visualizing the “star” pattern which was further placed in the sunlight at an interval of 24 h for 30 days. The images were shown in **Fig. S12**, indicating that the high fluorescence stability and durability of **CA**-CB[7] complex treated “star” pattern.

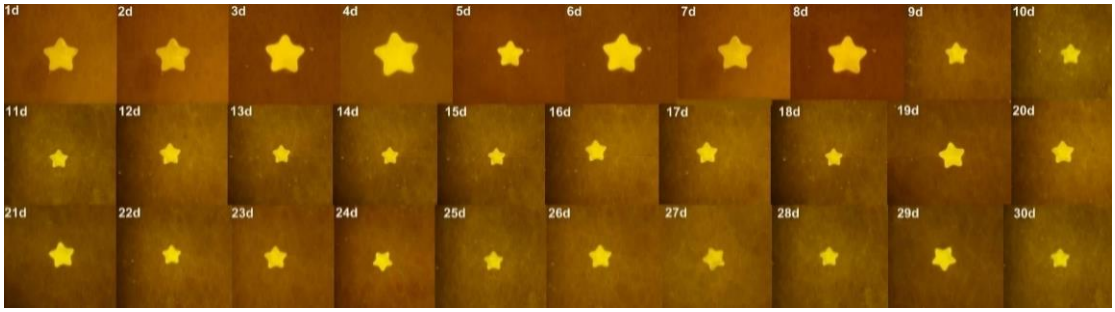

Figure S12. The stability and durability measurement of the "star" pattern visualized with **CA**-CB[7] system under exposing to the daylight (the experimental determination time is 30 days). The fluorescence pattern was imaged with photography after exposing to light every day.

A4 paper was cut into a "heart" pattern which was visualized by **CA**-CB[7] system. The "heart" pattern was washed with pure water for 6 times. And the fluorescence pattern was imaged with photography after rinsing every time. The results were shown in **Fig. S13**. Similarly, water was evenly sprayed around the "star" pattern visualized by **CA**-CB[7] system with an atomizer. The fluorescence pattern was imaged with photography after every spraying procedure. The results were shown in **Fig. S14**.

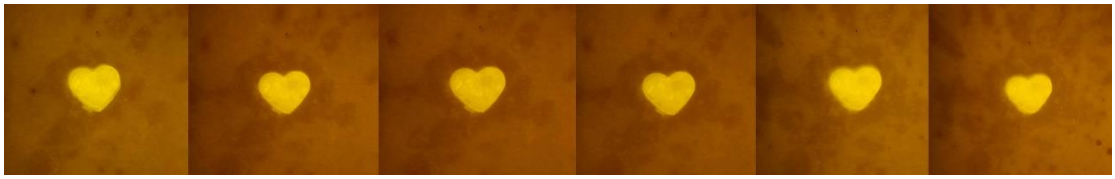

Figure S13. The stability and durability test were conducted for "heart" pattern visualized with **CA**-CB[7] system under the repeated rinsing procedure. The "heart" pattern was washed with pure water for 6 times. And the fluorescence pattern was imaged with photography after rinsing every time.

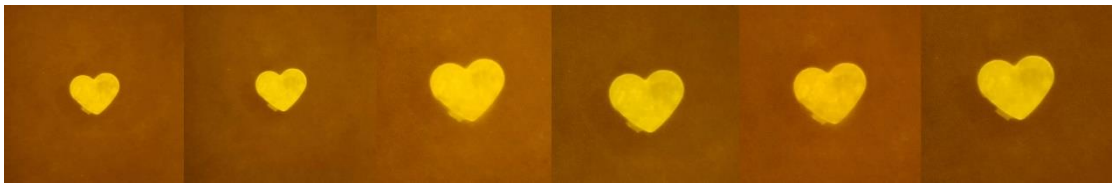

Figure S14. The stability and durability test were conducted by exposing the visualized

“star” pattern with **CA**-CB[7] system to humid environments (the humidity was increased by spraying water with atomizer). The fluorescence pattern was imaged with photography after exposing to the humidity environment every time.

A4 paper was cut into a “heart” pattern, which was visualized by **CA**-CB[7] system. Then the paper of “heart” pattern was treated with physical abrasion with fingers. The fluorescence pattern was imaged with photography after physical abrasion every time. The results were shown in **Fig. S15**.

Figure S15. The stability and durability test were conducted for the visualized “star” pattern with **CA**-CB[7] system after repeated physical abrasion for the paper. The fluorescence pattern was imaged with photography after physical abrasion every time.

The A4 paper was cut into a “star” pattern, which was visualized by **CA**-CB[7] system. The fluorescence pattern was irradiated with continuous irradiation with ultraviolet light (365nm). The fluorescence pattern was imaged with photography after irradiation every 30 min. The irradiation was lasted for 4.5 hours. The results were shown in Fig. S16. Similarly, the “star” pattern was exposed to the continuous irradiation with white light from LED lamp (30 W, 3.7 V). The fluorescence pattern was imaged with photography after irradiation every 30 min. The irradiation was lasted for 3.5 hours. The results were shown in **Fig. S17**.

.

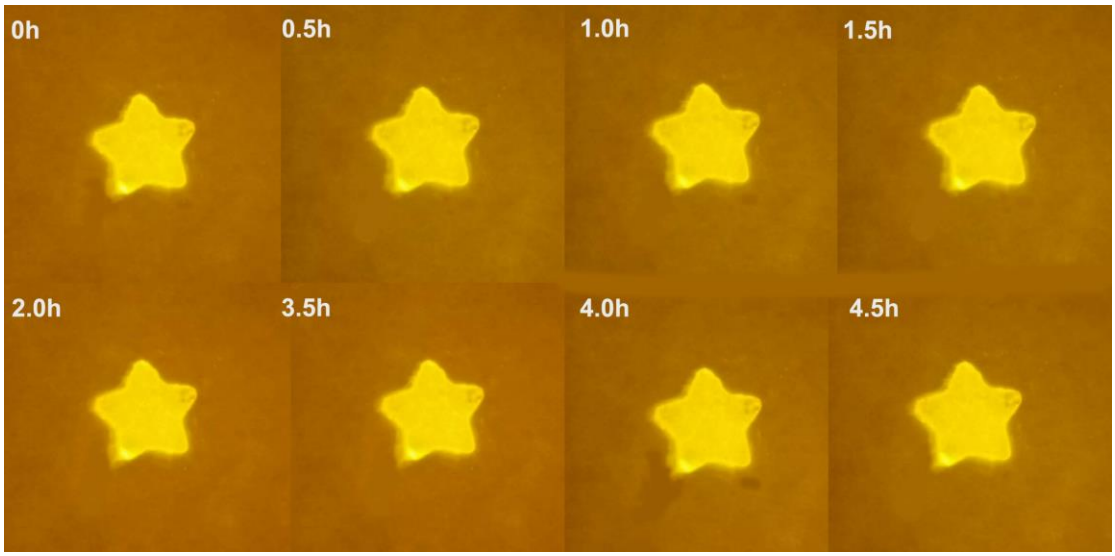

Figure S16. The fluorescence stability and durability test were conducted for "star" pattern visualized with **CA**-CB[7] system under the continuous irradiation with ultraviolet light (365nm). The fluorescence pattern was imaged with photography after irradiation every 30 min. The irradiation was lasted for 4.5 hours.

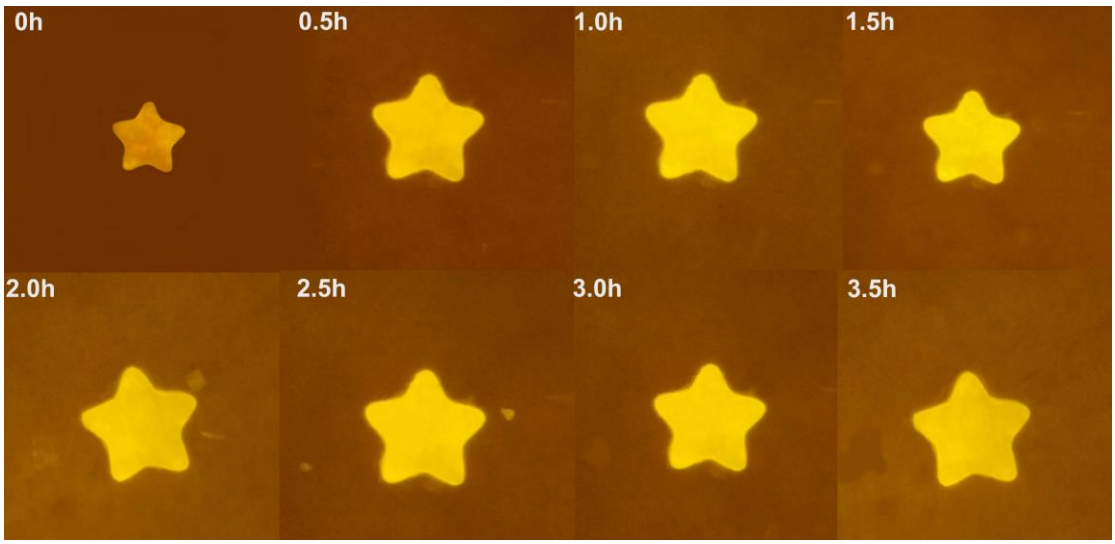

Figure S17. The fluorescence stability and durability test were conducted for "star" pattern visualized with **CA**-CB[7] system under the continuous irradiation with white light from LED lamp (30 W, 3.7 V). The fluorescence pattern was imaged with photography after irradiation every 30 min. The irradiation was lasted for 3.5 hours.

The A4 paper was cut into a "star" pattern, which was visualized by **CA**-CB[7] system.

The fluorescence pattern was kept under different temperature at 25 ºC, 40 ºC,60 ºC,80 ºC,100 ºC,120 ºC, respectively. Then, the fluorescence pattern was imaged with photography at very temperature.

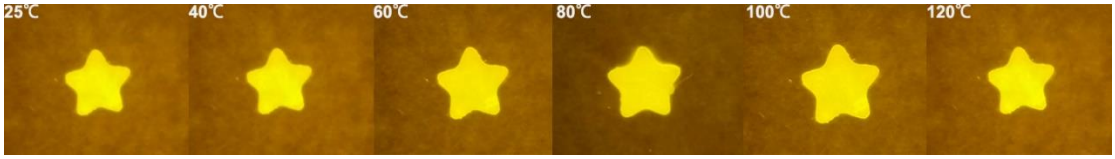

Figure S18. The fluorescence stability and durability test were conducted for "star" pattern visualized with **CA**-CB[7] system after the pattern was exposed to conditions with varying temperatures. The fluorescence patterns were imaged with photography after the temperature was at 25 ºC, 40 ºC, 60 ºC, 80 ºC, 100 ºC, and 120 ºC, respectively.

3.3 CA-CB [7] system was used for fluorescent anti-counterfeiting test on glossy coated paper

The "bear" pattern of the smooth glossy coated paper was soaked in **CA** solution first. After drying, no relevant pattern was found under the irradiation (left in Fig. S19). Then, the pattern was soaked again with CB[7] solution, and the relevant pattern showed a great fluorescence signal (middle in Fig. S19). After the treatment with amantadine hydrochloride, the fluorescence signal of "bear" pattern decreased. The results suggested that the fluorescence anti-counterfeiting effect of **CA**-CB[7] system is not limited to A4 paper.

Fig. S19 CA-CB[7] system was used for fluorescent anti-counterfeiting test on the glossy coated paper.

4. 2D NMR spectrum and NMR data analysis

We have conducted the HSQC and NOESY assay for **CA**. According to the ^{1}H NMR, ^{13}C NMR, HSQC, and NOESY spectra, **CA** totally has 14 C(sp^2)-H hybridized

hydrogen atoms, 1 C(sp^3)-H hybridized hydrogen atom (from hydrogen of N-CH_3-), 21 sp^2-hybridized carbon atoms (one is from the carbonyl group), 1 sp^3-hybridized carbon atom (from the methyl part of N-CH_3-). The detailed information of hydrogen and carbon signal was listed in the following. Particularly, **CA** contains 1 pyridine ring, 2 double bonds, 1 imidazole ring, and 1 naphthalene ring, and the carbonyl group and "N-CH_3-" part are located on the imidazole ring. The naphthalene ring and imidazole ring are connected by a double bond, which is E configuration based on the chemical shift (7.27 ppm) of the C(sp^2)-H hybridized hydrogen atom on the double bond due to the shielding region of the carbonyl group. The pyridine ring and imidazole ring are connected by a trans double bond that can be deduced from the coupling constant (J = 15.9 Hz) of the two C(sp^2)-H hybridized hydrogen atoms coupled to each other. One of the hydrogen atoms is 7.53 (1H, d, J = 15.8 Hz, H-9), and the other is 8.06 (1H, d, J = 15.8 Hz, H-10).

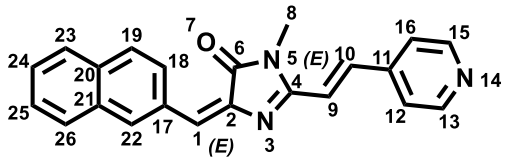

^{1}H NMR (DMSO-d_6, 400 MHz) δ_H 8.71 (1H, s, H-22), 8.69 (2H, d, J = 6.0 Hz, H-13, 15), 8.63 (1H, d, J = 8.8 Hz, H-18), 8.06 (1H, d, J = 15.6 Hz, H-10), 8.02 (1H, s, H-23), 7.98 (1H, d, J = 8.4 Hz, H-19), 7.94 (1H, d, J = 6.8 Hz, H-26), 7.86 (2H, d, J = 6.0 Hz, H-12, 16), 7.62-7.56 (2H, m, H-24, H-25), 7.53 (1H, d, J = 16 Hz, H-9), 7.26 (1H, s, H-1), 3.32 (3H, s, CH_3-8);
^{13}C NMR (DMSO-d_6, 101 MHz) δ_C 170.4 (s, C-6), 162.6 (s, C-4), 150.8 (d, C-13), 150.8 (d, C-15), 142.6 (d, C-12), 140.1 (s, C-11), 138.2 (d, C-10), 133.9 (s, C-21), 133.8 (d, C-12), 133.3 (s, C-20), 132.6 (s, C-17), 129.3 (d, C-23), 128.7 (d, C-18), 128.3 (d, C-19), 127.2 (d, C-24), 127.2 (d, C-26), 126.7 (d, C-25), 126.7 (d, C-1), 122.6 (d, C-12), 122.6 (d, C-16), 119.1 (d, C-9), 27.1 (q, C-8).

5. NMR Spectra and HRMS

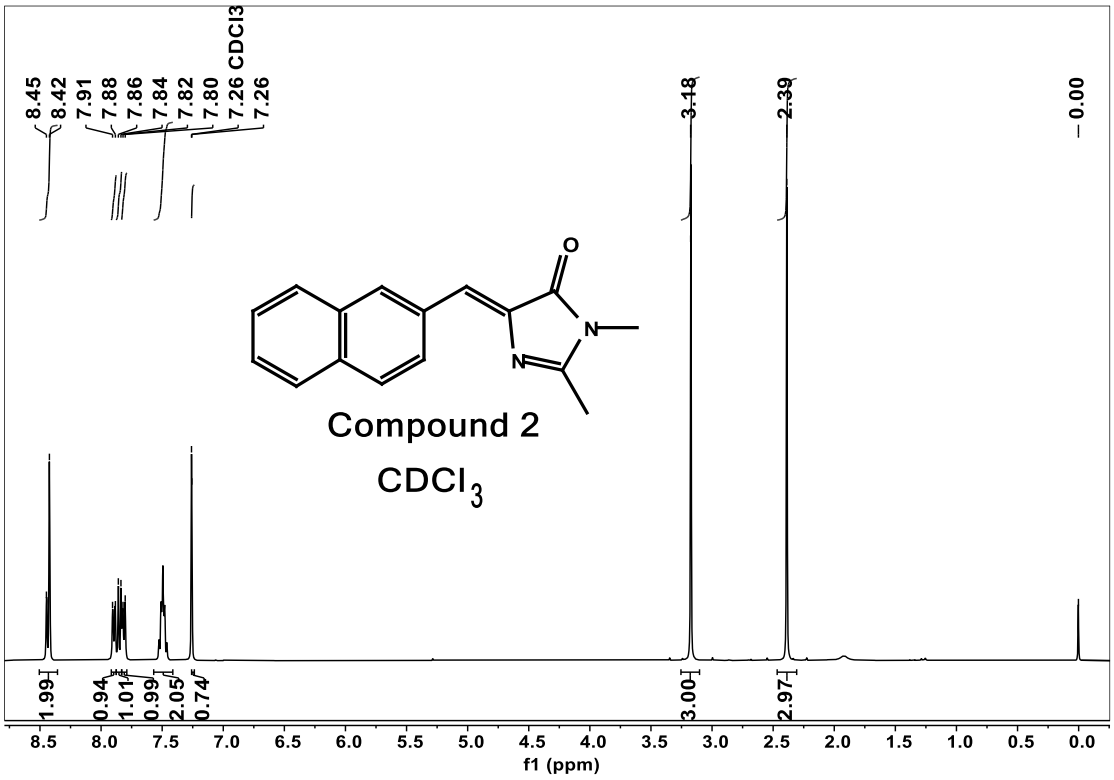

Fig. S20 ^{1}H NMR spectrum of compound 2.

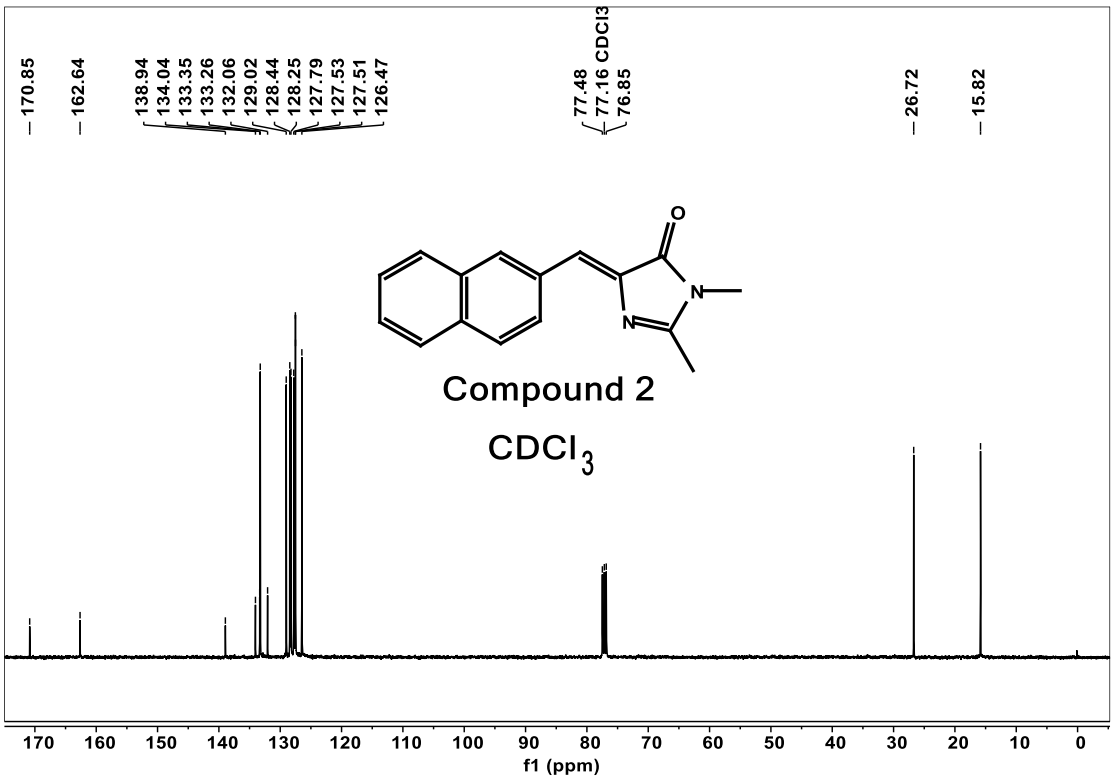

Fig. S21 ^{13}C NMR spectrum of compound 2.

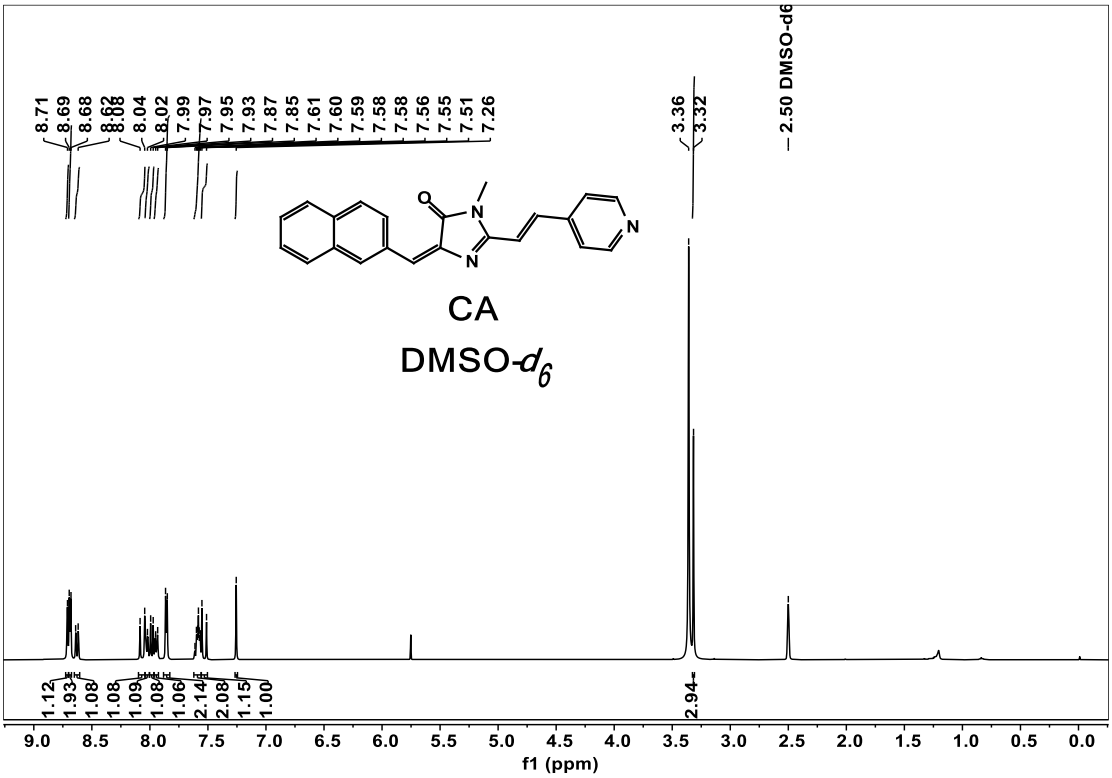

Fig. S22 ^{1}H NMR spectrum of **CA**.

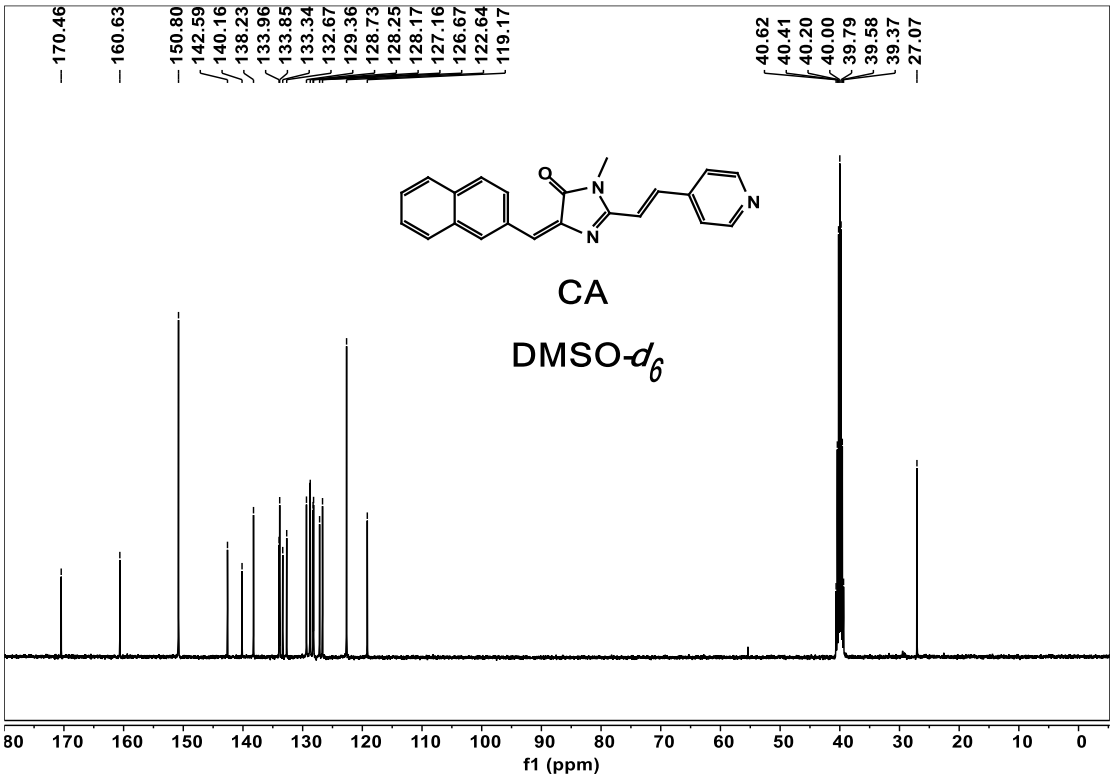

Fig. S23 ^{13}C NMR spectrum of **CA**.

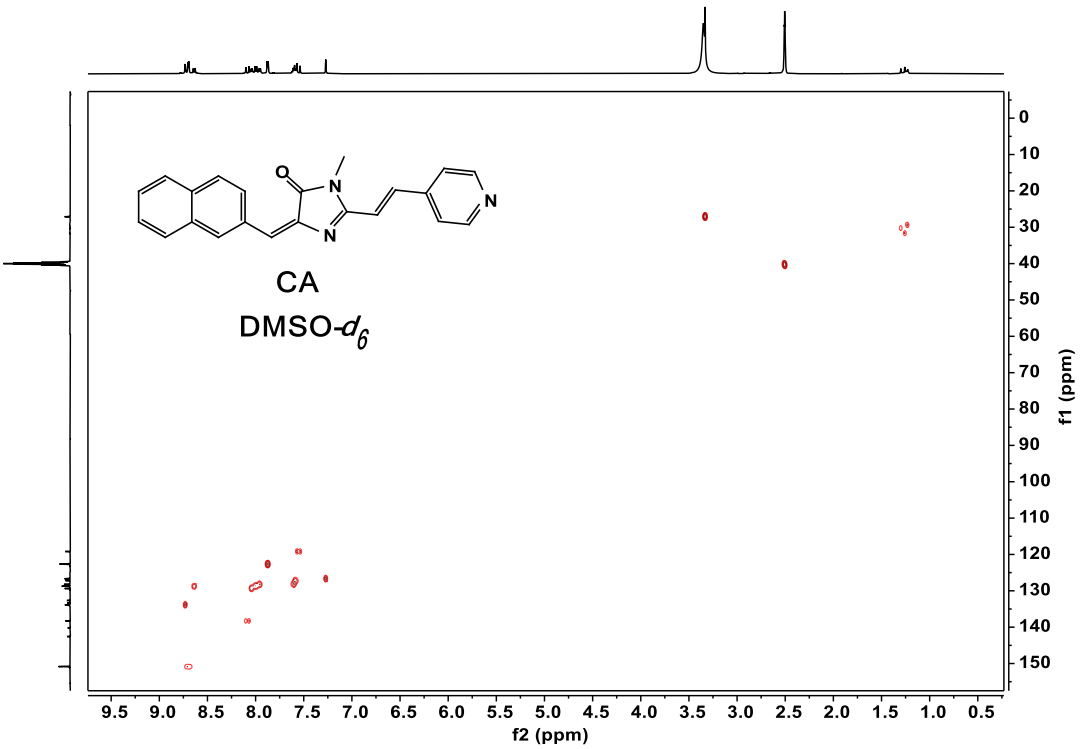

Fig. S24 HSQC spectrum of **CA**.

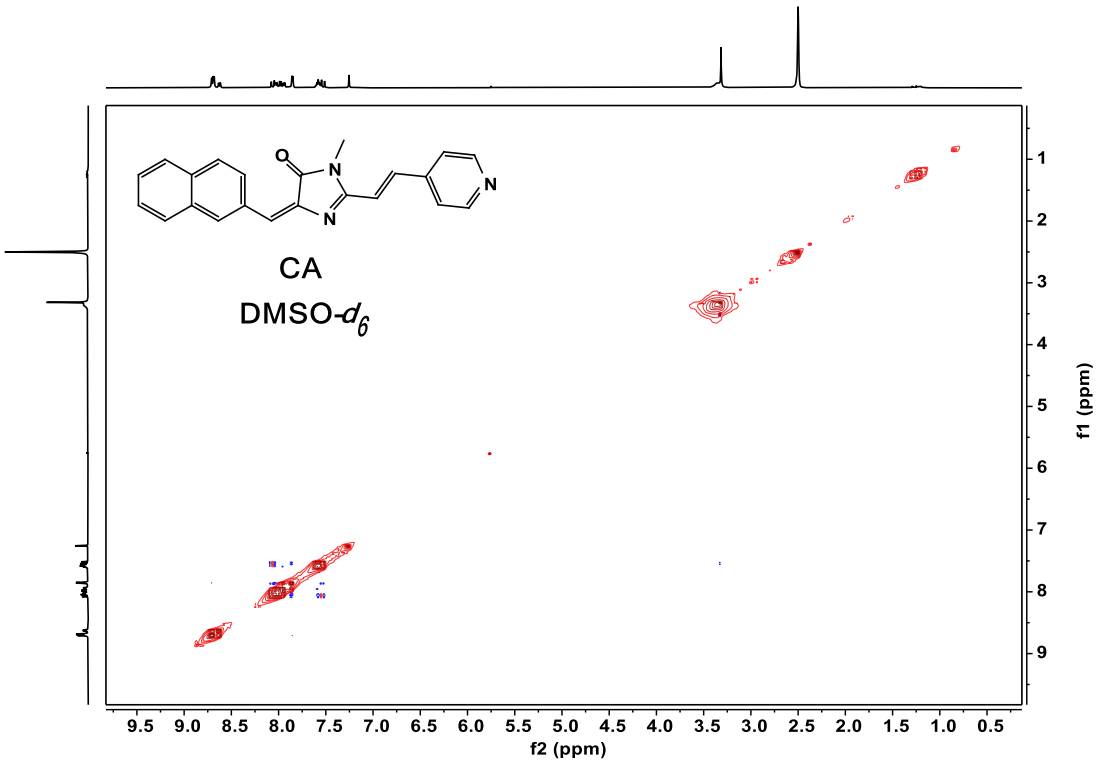

Fig. S25 NOESY spectrum of **CA**.

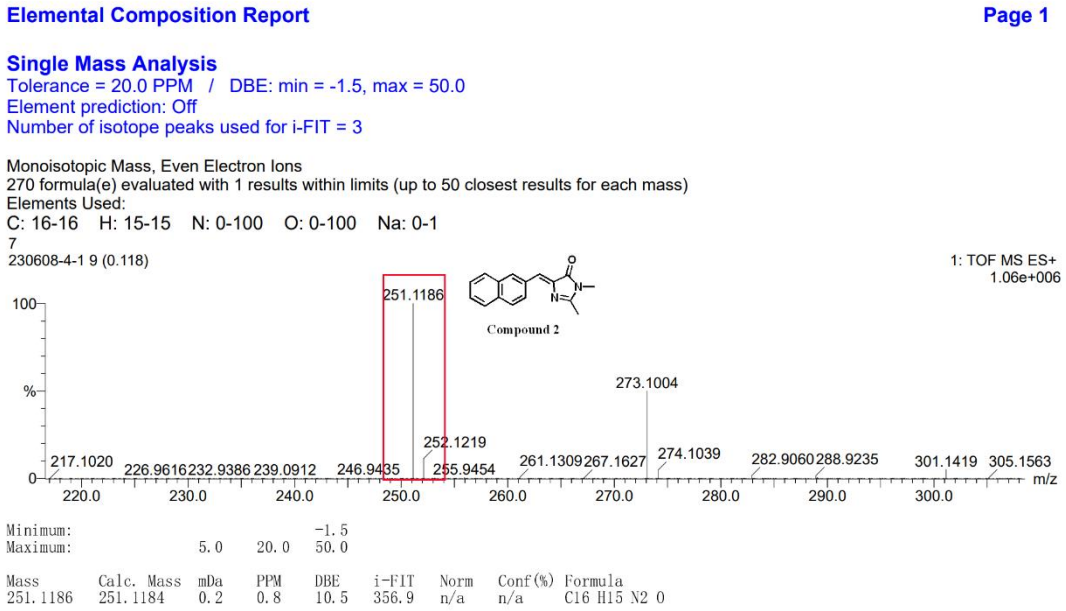

Fig. S26 HRMS of compound 2.

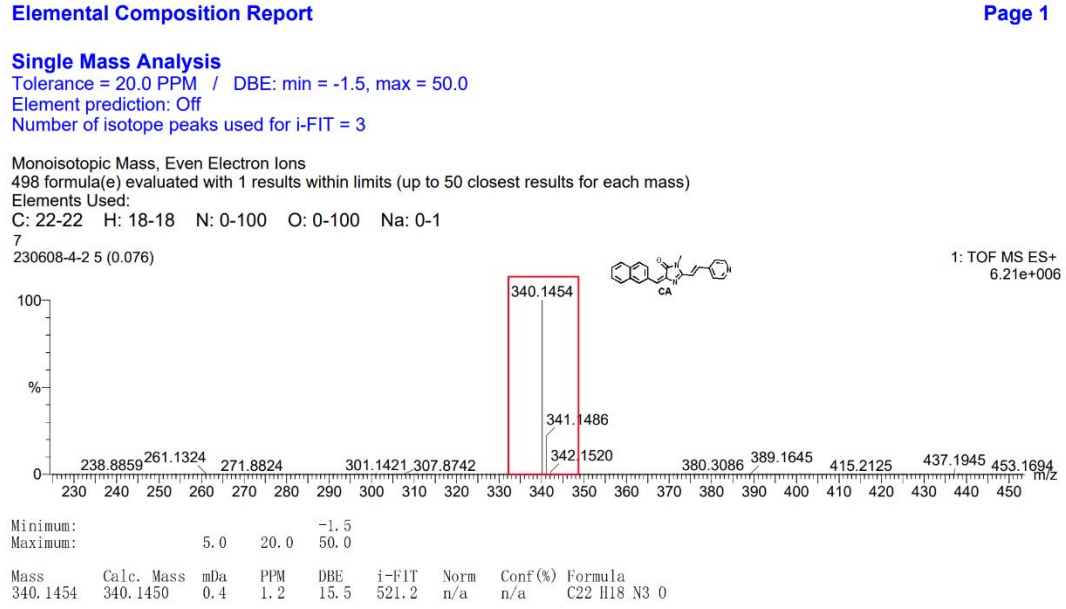

Fig. S27 HRMS of **CA**.

6. References:

1. N. Ruan, Q. Qiu, X. Wei, J. Liu, L. Wu, N. Jia, C. Huang and T. D. James, *J.Am.Chem.Soc*, 2024, **146**, 2072-2079.
2. S. Paul, R. S. Fernandes and N. Dey, *New J Chem*, 2022, **46**, 18973-18983.
3. N. Dey, B. Maji and S. Bhattacharya, *Chem Asian J*, 2018, **13**, 664-671.
4. D. Magde, R. Wong and P. G. Seybold, *Photochem. Photobiol*, 2002, **75**, 327-334.